Geoscience Frontiers 12 (2021) 101109

HOSTED BY

Contents lists available at ScienceDirect

Geoscience Frontiers

journal homepage: www.elsevier.com/locate/gsf

Research Paper

A new GIS-compatible methodology for visibility analysis in digital surface models of earth sites

Katerina Ruzickova *, Jan Ruzicka, Jan Bitta

VSB – Technical University of Ostrava, Czech Republic

ARTICLE INFO

Article history:
Received 28 June 2019
Received in revised form 11 September 2020
Accepted 12 November 2020

Available online 17 January 2021

Handling Editor: B. Pradhan

Keywords:
Digital surface model
Visibility analysis
Topographic data processing
Obstacle object
Permeability

ABSTRACT

As a GIS tool, visibility analysis is used in many areas to evaluate both visible and non-visible places. Visibility analysis builds on a digital surface model describing the terrain morphology, including the position and shapes of all objects that can sometimes act as visibility barriers. However, some barriers, for example vegetation, may be permeable to a certain degree. Despite extensive research and use of visibility analysis in different areas, standard GIS tools do not take permeability into account. This article presents a new method to calculate visibility through partly permeable obstacles. The method is based on a quasi-Monte Carlo simulation with 100 iterations of visibility calculation. Each iteration result represents 1% of vegetation permeability, which can thus range from 1% to 100% visibility behind vegetation obstacles. The main advantage of the method is greater accuracy of visibility results and easy implementation on any GIS software. The incorporation of the proposed method in GIS software would facilitate work in many fields, such as architecture, archaeology, radio communication, and the military.

1. Introduction

Visibility analysis is a widely used function in GIS (Wilson and Gallant, 2000). It identifies areas that can or cannot be seen from a single (or a set of) viewpoint(s). The clearly visible parts of an observer's surrounding area, as well as hidden parts, may thus be evaluated. Visibility analysis proves useful when selecting the best or optimal locations in urban studies (Hindsley et al., 2013; Kloucek et al., 2015), e.g., placement of various facilities which should be made visible (nice, interesting places) or those which should be rather hidden (e.g. wind turbines; Sunak and Madlener, 2016). Apart from architecture, visibility analysis is useful for tourism purposes (Brabyn, 2015), archaeology (Ogburn, 2006; Paliou, 2011; Supernant, 2014), communication engineering (propagation of radio waves; Klampfer et al., 2011), and may be highly serviceable in the military (Williamson and McLin, 2015).

Visibility analysis in standard geographic information systems takes inputs such as:

- the digital surface model (DSM) – raster layer, which continuously describes the surface elevation;
- the location of the observer – vector point location (X, Y, Z coordinates);
- the parameters determining the direction of view and the maximum visible distance.

Digital surface models are considered a category of digital terrain models (DTM) (Wilson and Gallant, 2000). While a DTM only describes the morphology of the terrain without its cover (buildings, vegetation, etc.), a DSM includes such objects (Li et al., 2005). DSMs may be obtained by acquiring all data at once using remote sensing. The advantage is that all objects (visibility obstacles) on the terrain are included automatically. However, the method does not allow work with the discrete objects. On the other hand, data on the terrain and data on objects (buildings and vegetation) can be obtained separately, thus leading to data combination in a DSM. This way, it is possible to pre-process qualitative information, such as vegetation permeability.

Site visibility under the canopy cannot be evaluated using standard visibility analysis in GIS due to the 2.5-dimensional (2.5D) geometry. Because 2.5D can use only one Z coordinate for one position (X, Y), a 2.5D DSM only represents the treetop parts but not the bottom parts. In addition to its shape, the position and permeability of the vegetation must be evaluated. The vegetation data should be handled separately (from the DSM data) for this purpose. Terrain, building, vegetation and other obstacles can be part of visibility processing when they are included in a digital surface model (DSM).

Conventional tools for visibility analysis are available in most GIS. They are mainly based on processing with the line-of-sight approach

* Corresponding author.
E-mail address: katerina.ruzickova@vsb.cz (K. Ruzickova).

https://doi.org/10.1016/j.gsf.2020.11.006

(El-Sheimy et al., 2005; Smith et al., 2007). In this approach, an imaginary connecting line (line-of-sight) is created between an observer's site and an observation target. In the direction of the line, a vertical profile of the surface is created, which is compared with a direct connecting line between the observer and the target. The comparison between the two lines divides the line-of-sight into visible and invisible portions, indicating whether the target is hidden by obstacles or not. Any invisible portion causes invisibility of the observation target. The line-of-sight approach is a point-to-point operation. But it may be computed from a single point to multiple destinations, providing a simplified picture of averal visibility from an observation point. During the calculation of visibility in all surrounding areas, each place in the surroundings progressively becomes the observation target. Using the line-of-sight method for each target eventually allows the evaluation of which surrounding places of the observer can or cannot be seen. The most described algorithms for viewshed are Xdraw, R2, R3, WS and RP (Kaucic and Zalik, 2002). There are two main concepts of visibility modelling: isovists and viewsheds (Smith et al., 2007).

Viewshed analysis concentrates on landscape, rather than on urban and architectural issues (Burrough, 1986). Viewshed analysis is basically calculation based on raster data (though algorithms using triangular irregular networks also exist; De Floriani et al., 1994, De Floriani and Magillo, 1999). It was introduced by Tandy (1967) using watershed analogy. Visibility is equivalent to shining a powerful light beam from an observation point and scanning around in a full circle. The tracing ray algorithm (e.g., at regular angular intervals) is applied to test the visibility between the observer point (vantage point) and the other pixels over a regular pixelisation grid (DSM) observer. A DSM requires a high-resolution image and takes considerable calculation time. A low-resolution image will lead to imprecise results. A viewshed produces an output raster with the same extent as an input raster. Software algorithms for viewshed delineation were improved, for example, by Lee and Stucky (1998), Kim et al. (2004), Bartie et al. (2010), Domingo-Santos et al. (2011), Chamberlain and Meitner (2013), and Yu et al. (2016).

An isovist is 'the set of all points visible from a given vantage point in space' (Benedikt, 1979). The evaluated points are usually the border points of the geometry of buildings in an urban area. Batty (2001) and Turner et al. (2001) have extended Benedikt's work. Isovists are naturally three-dimensional, but it can be studied in two dimensions – usually a horizontal section ('plan'). Vector data for outdoor visibility (isovists) was mentioned by Rana (2006). He developed a program, based on the ray tracing algorithm, that computes a visibility polygon which encloses the visible area (Wassim et al., 2011). Nijhuis et al. (2011) defined isovists as 'Isovits: sight field polygons or limit-of-vision plottings are the vector/based counterpart of viewsheds'. A first level of visibility can be implemented in an urban landscape. It allows optimal determination of the minimum number of target points to ensure complete coverage (Smith et al., 2007). A visibility graph is used for some applications, such as urban visibility of movement patterns in cities (Cooper, 2005; Natapov and Fisher-Gewirtzman, 2016).

The effect of vegetation permeability on visibility was theoretically described by Llobera (2007). He recommended replacing every tree with a set of very thin slices of a given transmissivity. The final visibility is calculated as the ratio of rays passing through all the slices. He also suggested a 3D representation of trees. These suggestions are reflected in Bartie et al. (2011), in which the authors also took into account visibility under bridges and overpasses. Seasonal vegetation changes and the decay in the atmosphere were incorporated, too. The method is based on the calculation of the visibility decrease rate caused by various influences.

Although convectional line-of-sight builds on two options only (visible and invisible places), objects may sometimes be partly seen behind vegetation. The main criticism of visibility analysis is that the binary output does not reflect the complexities of reality (Chapman, 2006). Some studies (Smith et al., 2007) have suggested diving the evaluated area into: almost certainly visible, possibly visible, possibly invisible and almost certainly invisible. A simple solution would be assigning a value between 0 and 1 to a partly visible place. However, this would introduce uncertainties into the final results. Other sources of uncertainty include the inaccuracy or complexity of the GIS data used (e.g., terrain model) and the seasonal character of vegetation as tree foliage affects the permeability rate. The basics of uncertain visibility analysis were set-up by Peter Fisher (1993), who also described the main factors that influence the visibility of surrounding areas (Caha and Rasova, 2015).

Uncertainty can be handled with fuzzy (Duraciova, 2014) or probabilistic solutions (Nackaerts et al., 1999). 'In essence the probable model of error allows us to determine the area which should be visible from a particular viewing point, while the fuzzy model tells us how distinct any object might be: the visible and the distinguishable locations.' (Fisher, 1993). Magoc et al. (2010) presented an algorithm that uses fuzzy integration to consider dependencies based on numerous criteria. These criteria can be the distance between the observer and the target, the time of the day, the position of the sun in the sky, the weather, and the vegetation density. When the line-of-sight goes through the vegetation, the rate of visibility decreases. Ogburn (2006) discussed a fuzzy reduction in the ability to recognise objects (of precisely known sizes) with increasing distances. Visibility reduction due to adverse environment conditions was studied as well (Wang et al., 2014). Visibility by the human eye and visibility by an advanced digital photogrammetric equipment were compared in various weather conditions.

Both approaches may be combined if we want to know which locations are visible and also distinguishable (Fisher, 1993). Arnot and Grant (1981) and De Floroani and Magillo (1997) investigated the possibility of including a DSM with different levels of accuracy to explain the concept of the view scale. The need to incorporate vegetation into visibility analysis was mentioned in studies by Lange (1990), Yang et al. (2007), and Liu et al. (2010).

The main problem of the conventional approach to visibility analysis is how to handle partial visibility of vegetation. None of the mentioned studies deal with it. In the probabilistic approach to uncertainty, researchers have presented algorithms that focus on elevation-error propagation into the results of a visibility analysis based, for example, on Monte-Carlo analysis (Nackaerts et al., 1999). Although these algorithms do not take vegetation permeability into account in their visibility analysis, the Monte-Carlo method seems to be a suitable method to model the influence of vegetation on visibility analysis, including its seasonal character.

Guth (2009) described various ways of acquiring and preparing vegetation data for visibility analysis. He compared the National Elevation Dataset of the United States, data from the Shuttle Radar Topography Mission (SRTM), vegetation inventories such as the National Land Cover Data, and LiDAR (light detection and ranging) data as suitable sources for visibility analysis, recommending LiDAR data as the best source. Raw LiDAR data can be used to categorize ground data and cover data, according to the shape and roughness of a given surface (Chang et al., 2008), with filtering methods. So, it is possible to detect continuous wood canopy (Coops et al., 2007) as well as individual trees (Chen et al., 2006). From airborne LiDAR measurement data, we can identify more parameters of objects that can obstruct visibility, including positions, shapes, types, etc. Some studies describe the use of multispectral or hyperspectral data for identification of selected tree species (Immitzer et al., 2012; Natural Resources Canada, 2015). In particular, the classification of coniferous and broadleaf trees was achieved with a high accuracy of 99.2% (Immitzer et al., 2012). For this classification, Immitzer et al. (2012) used the WorldView-2 image, 8 spectral bands, 50 cm for the panchromatic band and 200 cm for the multispectral bands. Just four standard bands were sufficient for the identification of the main four species. The accuracy of classification of all ten tree species was over 80% in this study. More elaborate data from airborne remote sensing allowed the examination of tree species in greater detail

(Zhang and Hu, 2012). Brandtberg (2007) worked on classifying individual tree species under leaf-off and leaf-on conditions using airborne LiDAR. The classification was focused on five deciduous and six coniferous species. Hence, some suitable sources and methods for this kind of analysis are available. Bartie et al. (2011) and Murgoitio et al. (2013) derived lodgepole pine tree obstruction permeability from the side-look scanning of a tree. Permeability was evaluated as the ratio of tree parts to the visible background behind the scanned trees. They also used the side view of the tree. But each tree was investigated individually, and thus the task was time-consuming.

To improve visibility analysis, the current paper presents a method that takes vegetation permeability into account. The method visibility analysis focuses on incorporating partially permeable obstacles using the Viewshed tool in ArcGIS. The novelty lies in the generalisation of a tree's shape and permeability. The approach is probabilistic since the results are focused on the visibility of locations (Fisher, 1993). It does not deal with the uncertainty of DSMs, as described in (Fisher, 1993), but is focused only on partial visibility via vegetation, based on the method described in (Bartie et al., 2011). This paper aims to describe the method in two study areas. The method is universal for different types of applications (in planning, architecture, archaeology, etc.). It is easy to implement in GIS tools because it uses the tools, which are available in all common GIS software.

2. Material and methods

The main idea of the new method is based on the fact that in the visibility analysis of a scene, some parts of the scene behind vegetation are visible while some parts are not visible. The amount of visible background is responsible for vegetation permeability. Vegetation permeability was managed during the quasi-Monte Carlo simulation, which repeats visibility analysis for all possible amount of vegetation permeability. The method is described in Section 3 (Results). It was implemented in ArcGIS. We used the Viewshed tool, because the viewshed functionality is more widely available in GIS software than the isovist functionality.

2.1. Study area and data

Two parts of the university campus (VSB – Technical University of Ostrava, Czech Republic) were chosen as the test study areas (Fig. 1). The university complex is in a suburb of the city of Ostrava, which has a population of 300,000 inhabitants. It is a relatively flat area, and is documented in Appendix A – Morphology of the study area. The building density is apparent from Fig. 1, with mainly 5-storey buildings. The nice scenery of the campus is partly made up of ornamental vegetation. There are coniferous (pine, fir, larch, spruce) and broadleaf trees (chestnut, birch, ash, oak, willow, lime tree, etc.), as well as bushes of various species and shapes (dogwood, symphoricarpos, rose, scrub pine).

For Site 1, the first modelled scene, data was processed in a raster format with a pixel size of 2 m × 2 m. We created a model of each tree and bush as a rectangular block of dimensions 2 m × 2 m and a specified height. Site 1 was used to confirm the designed algorithm (described later) – a verification of the relationship between the used vegetation permeability in the input and the degree of visibility behind the vegetation at the output. It was necessary to do this before solving the task in greater geometrical detail, where the verification could be more complicated.

The second location, Site 2, was processed over the rasters with a pixel size of 0.5 m × 0.5 m. It allowed us to create more detailed geometrical models of vegetation, which is described later in Section 2.2 (vegetation data pre-processing).

Site 1 was selected because of a narrow view through the corridor of trees, which is a pathway bounded by a line of trees on either side. The

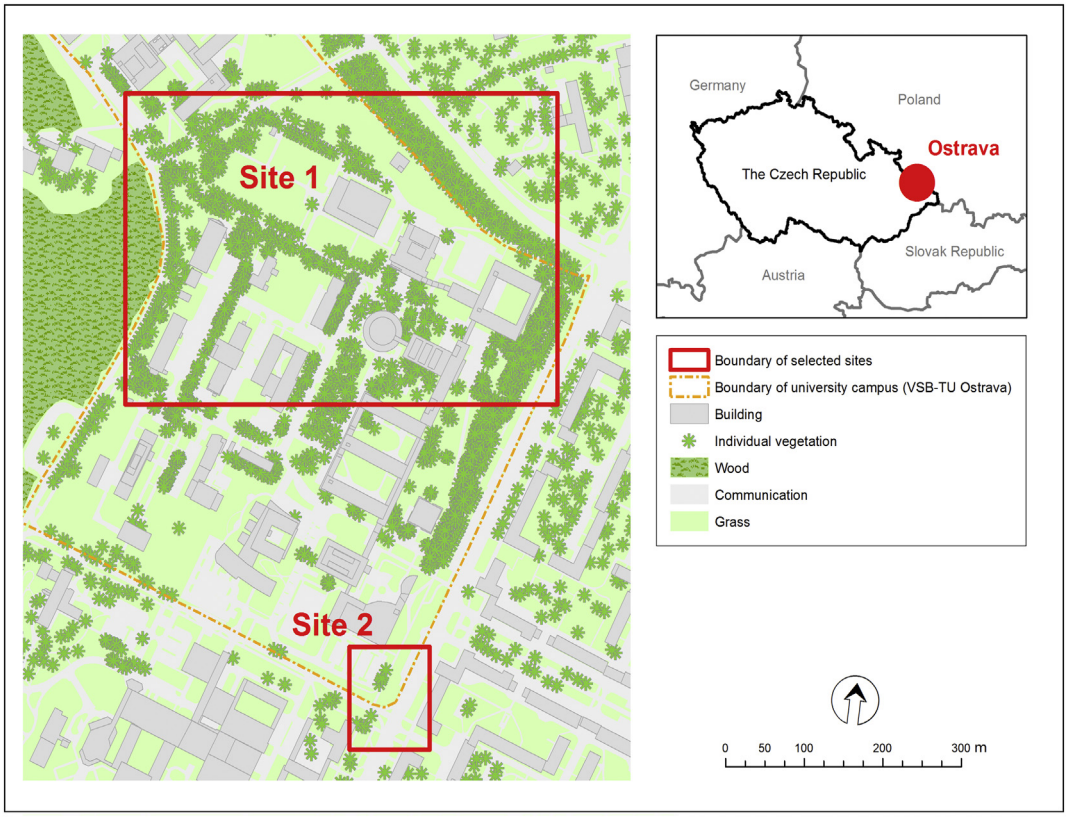

Fig. 1. Map of the study areas on the university campus (VSB – Technical University of Ostrava, Czech Republic). Site 1 is solved using a spatial resolution of a 2 m pixel size and Site 2 with a resolution 0.5 m × 0.5 m.

observer site is near the line of trees with high buildings behind them. It was necessary to pre-test the effect of using and omitting the vegetation data during visibility analysis. To avoid long-winded calculations, we focused on details with smaller areas afterwards. Finally, we chose a different part of the university campus with not so many trees and which offered a wider view. At this site, we could observe better partial overlapping of the trees which was not clearly noticeable in Site 1 (where there was full overlapping of the trees).

More detailed and real data and values were used afterwards. These were prepared for Site 2.

To obtain rough background visibility, the designed method was applied on the whole area depicted in Fig. 1 (not just Site 1). In this case, the same input data resolution as for Site 1 was used.

Data were obtained from the university data inventory. They were acquired mainly by students, especially the positions, heights, species of trees and bushes, and elevation data. Building datasets were based on technical reports. All the datasets were in a vector format.

2.2. Vegetation data pre-processing

The vegetation layer for this study contained the locations of trees and bushes with their attributes. The location of trees and bushes was set as a centre point and the accompanying attributes were their heights, diameters and species. Tree and bush positions were acquired by geodetic backward measurements and polar method (with total station TOPCON GPT-7001), so the accuracy was precise (mean error 14 cm). The height of the vegetation was measured as a trigonometrically determined elevation and a tape measure was used to determine the vegetation diameter.

Our first step in this study was to obtain data about vegetation permeability. The permeability parameter of each tree or bush was not acquired separately. Instead, a table of typical parameters of permeability for each type of vegetation was prepared. The permeability values for the winter season and the rest of the year were quantified separately. This separate quantification was important because of changing tree foliage during the year. A description of the method used for the quantification follows. The database of the permeability of tree species was built only for selected species present in the testing area. It consists of about 50 species (types). For each of the species, the permeability was evaluated as the average transparencies of a few vegetation delegates of this species. Approximately ten winter images and ten summer images of vegetation delegates were used for each of the species. The tree must be photographed from the ground (or from a place close to the ground). Pixels of vegetation pictures were separated into vegetation and background categories with a supervised maximum likelihood classification (ESRI, 2016). The permeability of each tree or bush was then calculated as the number of background pixels divided by the number of pixels that the tree or bush represents in the rectangle. This approach is similar to that of (Bartie et al., 2011), but its manner of data collection is faster because it is not necessary to acquire data in the field for each study separately. Once a database of parameters for vegetation species has been created, it can be used repeatedly.

Then the permeability values were linked to the vegetation in the vegetation dataset. The tables were joined through the vegetation type. All necessary attributes of the vegetation were there. Each tree or bush in the point layer dataset has its own value of height, diameter and permeability.

Afterwards, the vegetation geometry was also processed. At Site 2, each plant was processed as follows (see also Fig. 2):

(i) To simulate the vegetation diameter for point vegetation representation, a multiple buffer was created around vegetation locations. This means that circular distance zones were created round the vegetation points (ESRI, 2019; Fig. 2). The maximum range was set according to the vegetation's width (diameter).

(ii) Multi-buffers (distance zones) were converted into two rasters – a raster of vegetation heights and a raster of vegetation permeability. The pixel values were taken from the attributes of vegetation heights and permeability. The maximum value of the height and permeability was in the centre of the tree or bush. In cases of buffer overlaps, the highest value of height and the reduced value of permeability were used.

Site 2 was processed with a resolution 0.5 m × 0.5 m, but Site 1 was solved in a spatial resolution of 2 m pixel size. So, the vegetation was pre-processed in a more generalized form for Site 1. The vegetation was presented just as a rectangular block with a specified height and one value of permeability for a whole tree or bush in this case.

2.3. Surface elevation data pre-processing

The data for the surface model were obtained from airborne remote sensing and ground measurements. Stereo pairs of aerial survey photos were processed on Erdas software to evaluate terrain heights. The remote sensing dataset contains the irregular elevation point network, with a point-spacing of 5–20 m. These points were completed with precise 3D hardlines in artificially rebuilt parts of the terrain. The hardlines were acquired by ground measurements (GPS-RTK and geodetic measurements – levelling line) and show the edges (borders) of roads, pavements, parking sites and building footprints, the features arising from urban activities in the area of interest. This allowed the inclusion of the local characteristic shapes of the terrain. The DTM was created as a 2.5D model. A TIN (triangular irregular network) model was created first and then it was converted into rasters (with a resolution 0.5 m × 0.5 m for Site 2 and 2 m × 2 m for Site 1). A map of the DTM and its morphology can be seen in Appendix A.

Then, two DSMs for each location were created: a DSM without vegetation (only opaque obstacles presented, e.g. buildings) and a DSM with vegetation (opaque and partly permeable obstacles presented together). To create the DSM without vegetation, a raster of building heights was added to the terrain. To create the DSM with vegetation, a raster of vegetation heights was utilised. (Fig. 2 and Appendix B).

- DSM without vegetation = 2.5D DTM + 2.5D model of buildings
- DSM with vegetation = 2.5D DTM + 2.5D model of buildings + 2.5D model of vegetation

3. Results

3.1. A new methodology for visibility analysis

The visibility calculation was based on a quasi-Monte Carlo modelling method with pseudo-random values. The Monte Carlo method is based on repeating the problem simulation many times with some randomly changing parts of the input. All the results are processed afterwards to get the required output. The prefix 'quasi' means that although the method is based on the Monte Carlo method, it is modified. The modification lies in a generation not of random values in the input but of pseudo-random values. In this case, we used an increasing numerical series from 1 to 100 (which represents 0–99% of the processed permeability).

For each one percent of permeability in the range of 0–99%, one variation of visibility was calculated. The first variation processed the influence of vegetation with a 0% permeability. The second variation (repeating) processed the influence of vegetation with a 1% permeability, and so on (Figs. 3, 4).

The final visibility based on vegetation can be described with a simple eq. (1):

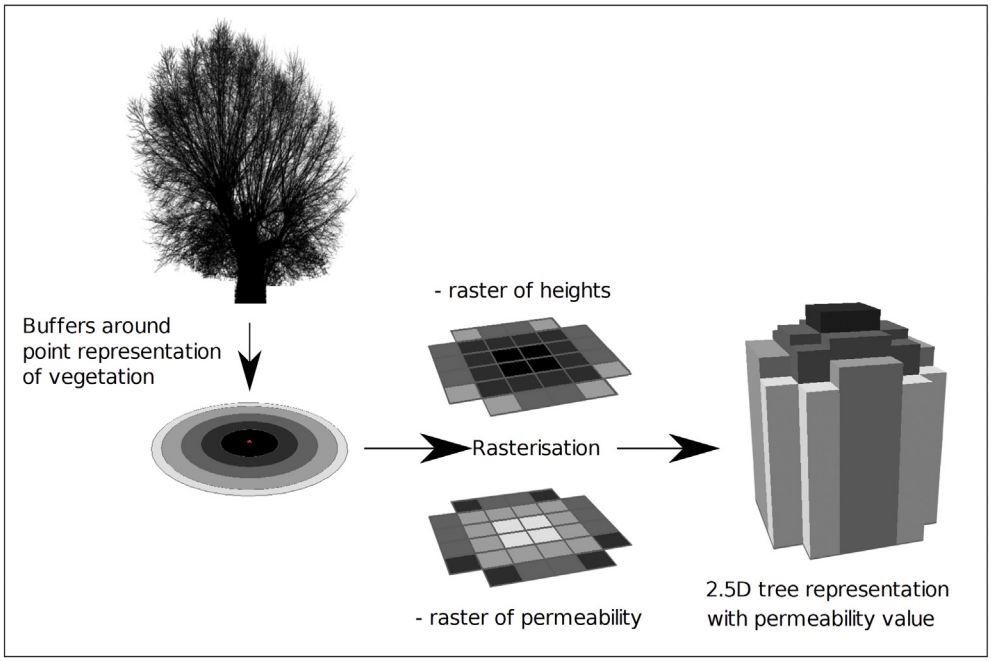

Fig. 2. Vegetation data processing. 2.5D vegetation representation and a raster of vegetation permeability are created form point vegetation data and vegetation attributes (diameter, height and permeability).

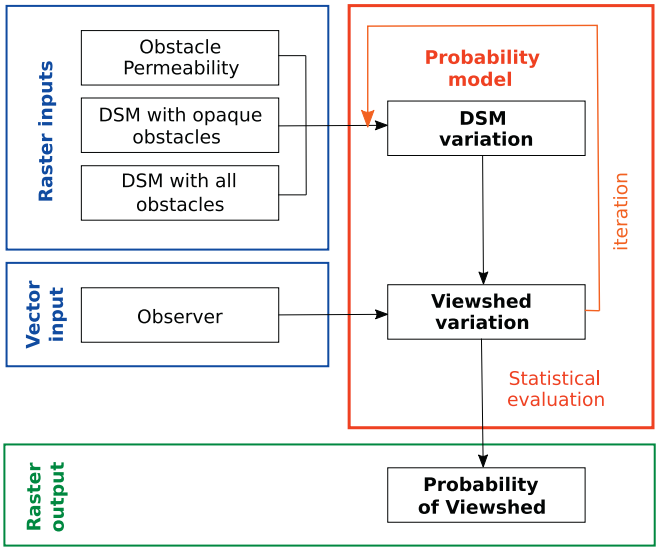

Fig. 3. Schema of a viewshed model based on a quasi-Monte Carlo simulation.

$$p(x_{ij}) = \sum_{k=1}^{100} x_{ijk} \quad (1)$$

where $p(x_{ij})$ is the probability of visibility of a cell at the i^{th} row and j^{th} column in percent; and x_{ijk} is the visibility over surface with vegetation permeability $< k$ encoded in binary mode (0: not visible or 1: visible), with k ranging from 1 to 100.

A different layer, 'DSM variation', was prepared according to the amount of processed permeability for each repetition. Values of 'DSM variation' were a combination values from the layers 'DSM with vegetation' and 'DSM without vegetation'. Specifically, the selection, from which layer the values came, was based on the condition that the value of vegetation permeability should be less than the iteration number. In pixels where the condition was fulfilled, the layer 'DSM variation' got its values from the layer 'DSM with vegetation'. In pixels where the condition failed, the pixel values from the layer 'DSM without vegetation' were taken for 'DSM variation'. This approach ensured that only some of the permeable obstacles (for the actually processed amount of permeability) were used. So, for the first iteration, it was tested if the pixels in a layer of obstacle permeability had values less than 1 (so all pixels with vegetation of opacity 100% were incorporated into the DSM). In the second repetition, the selection of pixels for 'DSM variation' was set with the condition that the permeability value at the pixel site in a layer of vegetation must be less than 2 (so all pixels with vegetation of opacity 100% or 99% were incorporated into the DSM). Generally, opaque obstacles like terrain shapes and buildings are always part of 'DSM variation'. Permeable obstacles like trees and bushes are added incorporated into 'DSM variation' only according to the condition mentioned above.

During repetitions, visibility analysis from a specified point over all calculations is performed upon updated 'DSM variation'. There are, thus, 100 variants of visibility when the repetition is completed. Each variation in resultant visibility is influenced by a different number of permeable obstacles. All variations of visibility together provide information about how many times it is possible to see through the vegetation. These values are used as the probable visibility behind vegetation obstacles.

The iterations of calculation are described in Fig. 4 with a simple flat DSM, so the only obstacle is vegetation.

The new methodology was implemented in ArcGIS Appendix C and Python script.

The following algorithm was used:

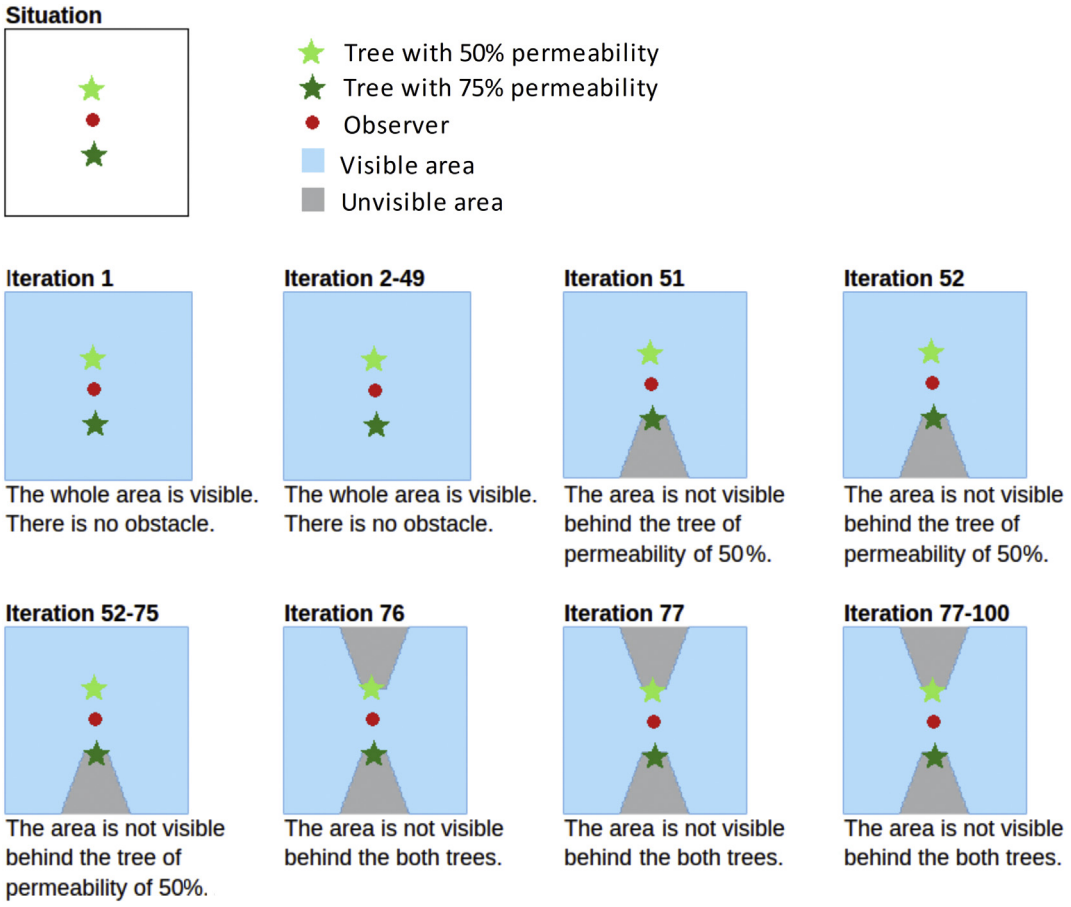

Fig. 4. Iterations of calculation.

For 0 to 99 do:

If (Obstacles Permeability Pixel Value > Iteration number) *then* DSM variation Pixel Value = DSM with opaque obstacles Pixel Value

else DSM variation Pixel Value = DSM with all obstacles Pixel Value

Viewshed calculation

Sum of Viewshed variations

The method may be extended with an uncertainty in the DSM and an uncertainty in vegetation permeability, as described in (Fisher, 1993). Therefore, for each iteration of the computation, a set of iterations may be introduced to simulate error propagation in the DSM, vegetation height, vegetation width and vegetation permeability uncertainty. All parameters may be simulated by the Monte Carlo approach.

$$p(x_{ij}) = \sum_{k=1}^{100}\left(\frac{\sum_{l=1}^{q}\sum_{m=1}^{r}\sum_{n=1}^{s}\sum_{o=1}^{t}x_{ijklmno}}{l+m+n+o}\right) \quad (2)$$

where $p(x_{ij})$ is the probability of visibility of a cell at the i^{th} row and j^{th} column in percent; and $x_{ijklmno}$ is the visibility over the surface with vegetation permeability $< k$, elevation realization l, realization m of width of vegetation, realization n of height of vegetation, and realization o of vegetation permeability, encoded in binary mode (0: not visible or 1: visible), where k ranges from 1 to 100.

This extension will increase computational time, but allows for better simulation of uncertainty in the data. The database of permeability of vegetation must be extended with information about error distribution for this purpose.

The method may be extended with fuzzy approach if it is required to distinguish locations as well. For this purpose, all equations described in (Fisher, 1993) may be considered. Such an extension will have a rapid impact on the speed of the algorithm.

3.2. Visibility calculation at the study area

The first test of the method was done on Site 1. The observer was on the pathway bounded by lines of trees (Fig. 5 – Observer position). The

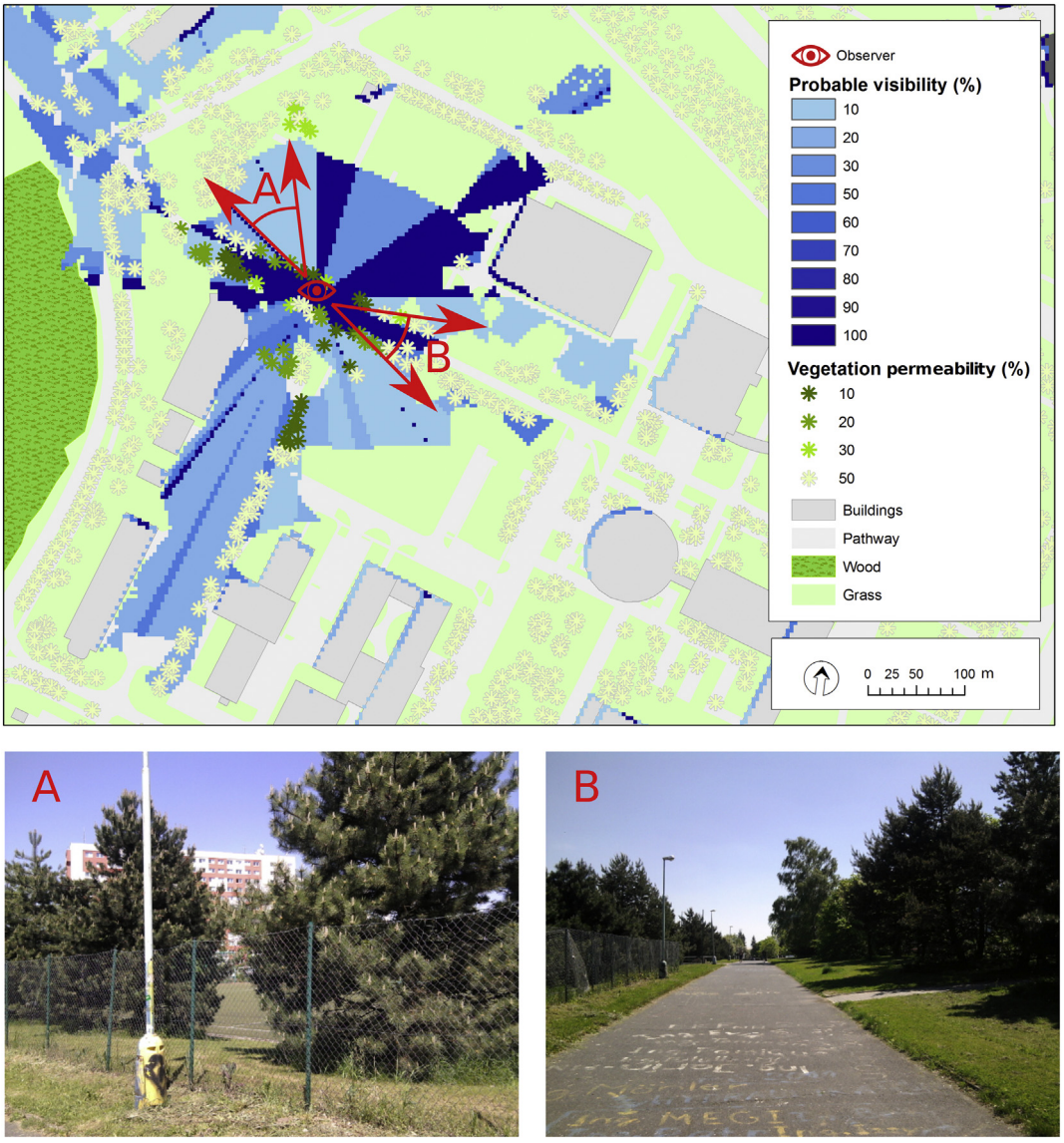

Fig. 5. Visual comparison of results for the designed method (Site 1) and site photographs. Red arrows (in map) show the direction of view from the observer's site (from which two photographs were taken).

first tests of the method were successful. The original algorithm of the Viewshed tool provided a reduction in visibility caused by surface topography (terrain curvature and buildings), and our added algorithm decreased the rate of visibility caused by vegetation permeability (Fig. 5) in the right degree. It means that an area behind a 20% permeable tree can be seen with a 20% probability. The darkest blue (in Fig. 5) represents the area which was visible without any limitation. The lighter blue represents the area where the visibility was affected (reduced) by vegetation. Places which could not be seen from the observer's location are not filled in the figure. So it is possible to see the topographic background. Visibility boundaries perpendicular to the view direction are caused by the terrain morphology.

Fig. 5 also shows two photographs taken from the observer site. The red arrows (in the map above) show the direction of view from the observer's position, which was used for taking the photographs. The clear visibility above the pathway can be seen in the picture on the right photograph B. The pathway is surrounded by trees which block (or decreased) the visibility of the surroundings. The left photograph A presents the visibility between the trees which do not completely obscure the building behind them.

Table 1
Results of visibility calculation with different vegetation influence. Below are the results of three options of dealing with vegetation during visibility analysis in rows. Ratios of 100% visible, partly visible (1%–99%), and non-visible area were evaluated for each option.

Calculation type	100% visible area (%)	Partly visible area (%)	Non-visible area (%)
Visibility without vegetation influence	17.3	-	82.7
Visibility with vegetation acting like an opaque barrier	3.4	-	96.6
Visibility with vegetation acting as a permeable barrier	3.4	14.4	82.2

To compare the effect of using or omitting the vegetation data during visibility analysis, two other common visibility calculations were done (Table 1). The first calculation omits vegetation. The second calculation counts vegetation as opaque barriers. When the vegetation was not considered, about 17% of the area was evaluated as clear view (Table 1). But in reality, part of it was hidden by vegetation. When the vegetation was set as an opaque barrier, this partly hidden area was added to the non-visible area; however, some parts of it were evaluated as partially visible (14%). This can be seen from the visibility evaluation when the vegetation is used as a permeable barrier. This evaluation (ratios of visibility) is site-dependent. But the effect that a partly hidden area could be incorrectly put into a fully visible or fully invisible area during common visibility analysis is valid in general.

The calculation was also tested in greater detail at Site 2 (Appendix D). Each tree was modelled as a group of pixels according to its height and diameter (Fig. 2). Fig. 6 illustrates the side view which can be presented to an ordinary user.

Different cartographic presentation was made for different users. The focus of the presentation was changed from a visible area to an invisible area. The result values of visibility were inverted. In this context, the probable visibility was renamed the rate of visibility reduction. The lowest value of probable visibility (Fig. 5) corresponds to the highest value of visibility reduction (Fig. 6). The highest value of probable visibility (Fig. 5) corresponds to the lowest value of visibility reduction (Fig. 6). Also, the manner of scale description in the picture result was changed. There is only a continuous scale from higher to lower visibility reduction. This is a vaguer presentation of the results, but it respects the rules for the visualisation of uncertain results. The present precise values of the results are not suitable, because there was a generalisation of tree shapes and their permeability in our method. So the results cannot exactly respect the real state of visibility. That is why the legend in the picture has been adapted.

The results were checked visually in the terrain. Verification of viewshed analysis can be based on panoramatic photographs (Arnot and Grant, 1981; De Floroani and Magillo, 1997; Sarnowski et al., 2018), where the viewshed content is compared with the content of the panoramatic photograps taken from the observer site (in reference ponits). We used an analogous method – comparison with reality. There was the possibility of classification into only 3 situations: whole visible buildings, partly visible buildings behind the vegetation, and invisible buildings. The results were 95% correct in this field of view. The inaccuracy of result was as a result of the accuracy of vegetation geometry. We did not examine the degree of the viewshed reduction because of the geometrical (dimension) task reduction to 2.5D. In a 3D task, supervised maximum likelihood classification (ESRI, 2016) can be used, but this will be distorted in a 2.5D task. We could not evaluate which parts of a building that were seen. When a (high) building was evaluated as visible, only the upper part could be seen, since the lower part might be hidden behind trees. This, however, is not noticeable from the results.

The algorithm is deterministic and the view of a tree with 20% permeability causes an 80% visibility reduction behind the tree. The algorithm is valid in this view. But we introduced some uncertainty into the evaluation via a generalisation of the tree models. We set the representative value of vegetation permeability for each type of vegetation according to approximately 10 examples of each type. So, we suppressed the diversity of particular examples of each vegetation type. This led to deviations in the results which could be barely evaluated (as other visibility studies shown, e.g., Bartie et al. (2011) and Murgoitio et al. (2013)).

4. Discussion

Incorporating vegetation into visibility analysis is very important although for a long-time previous studies tended to neglect vegetation data. The visibility of 14% of the surroundings was affected by vegetation at our study area (Study area 2). Some parts were hidden completely and some partly. There is no doubt that partial visibility is valuable too.

The most precise and complex data should lead to the best results of visibility analysis. Vegetation, as one feature that obstructs visibility, should be described with parameters like the vegetation position, the shape of the tree or bush, and the vegetation permeability. But the shape and permeability of a tree (or bush) varies from one occurrence to another. There is no doubt that methods used by Bartie et al. (2011) and Murgoitio et al. (2013) to acquire the parameters of vegetation are very useful. On the other hand, they are very time-consuming and require a lot of site works. Using common vegetation inventories, we usually get only information about vegetation position, species, age and health. Next parameter - the height of vegetation can be obtained by taking the difference between surface and terrain model. We could not get information about vegetation shape and permeability. Our database of these parameters assigned to vegetation species will likely save time with making and processing site photos. We were conscious of reduction in the individuality of the vegetation.

The dimensionality of the geometry of the model also influences the visibility results. Our world is 3D in geometrical view. The designed algorithm works with 2.5D data only. This introduces some limitations during visibility evaluation. It is not possible to process correctly the

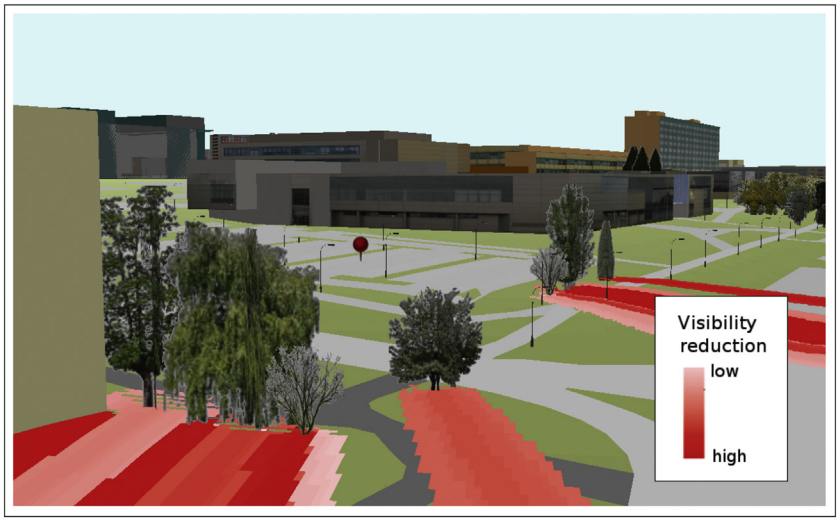

Fig. 6. Side view of visibility analysis results with real data (Site 2).

space under a tree crown, because it is always modelled as a part filled in by a tree, where there could be an open space there in reality. Data for 3D tree model construction are still not commonly (and freely) available. Using 2.5D data helps to decrease the data volume and speed up the calculation. One big advantage of using 2.5D data is the possibility it offers of using a common GIS viewshed function which works over the DSM raster data.

In comparison to the methods in some of the studies mentioned (in Section 1 – Introduction), the new method simplifies the evaluation of the variability of vegetation permeability. The simplification consists in establishing typical models for each type of trees and bushes. This leads to a reduction in the variability of vegetation objects, but allows for the processing of a wider area and quicker computation. A higher variability and complexity of vegetation parameters should help, but it may bring higher demands on vegetation data acquisition and permeability evaluation. Such a solution can be used only in particular, pre-selected small areas. For a wider and simpler calculation, a more universal approach is suitable.

Another problematic part of the proposed algorithm concerns the handling of trees that are in the same line of sight. The algorithm does not deal with this situation. However, this limitation should not matter much. According to Llobera (2007), visibility behind trees that are in the line of sight decreases exponentially. The most important issue is the influence of the first vegetation obstacles in front.

5. Conclusion

The method developed in this article allows the incorporation of vegetation permeability data into visibility analysis. The method introduces a more general and easier way to pre-process vegetation data as well. It has some limitations, but it offers one universal approach to a wide range of uses. The results describe the probable visibility or non-visibility behind given obstacles, which corresponds to the probable permeability of the obstacles. The proposed algorithm can be used in any GIS software that can calculate viewshed for 2.5D geodata.

Declaration of Competing Interest

The authors declare that they have no known competing financial interests or personal relationships that could have appeared to influence the work reported in this paper.

Acknowledgement

This work was financially supported by project 133/2016/RPP-TO - 1/b "Teaching of advanced techniques for geodata processing for follow-up study of geoinformatics". The authors wish to thank Mrs. Gabriela Chudasova, Alena Kasparkova, Mr. Mark Landry and City Hills Proofreading for proofreading the manuscript.

Appendix A. Morphology of the study area

The profile curvature is delimiting convex (negative values) and concave (positive values) shapes. The absolute value of the curvature reports the rate of curvature. Higher values are more curved. Local hardlines, such as road edges, pavements, and elevation transitions between the terrain and the buildings, can be seen more conspicuously for such more curved places because they have extreme values of curvature. For visibility evaluation, places with higher negative values of profile curvature are important. These include the convex shapes of terrain – smaller or bigger backs of hills (or small elevation humps). They can act as local visibility horizons, which hide a part of the terrain behind them. The higher positive values of the profile curvature represent a concave terrain shape (terrain depression). The profile curvature values of flat terrain are around zero.

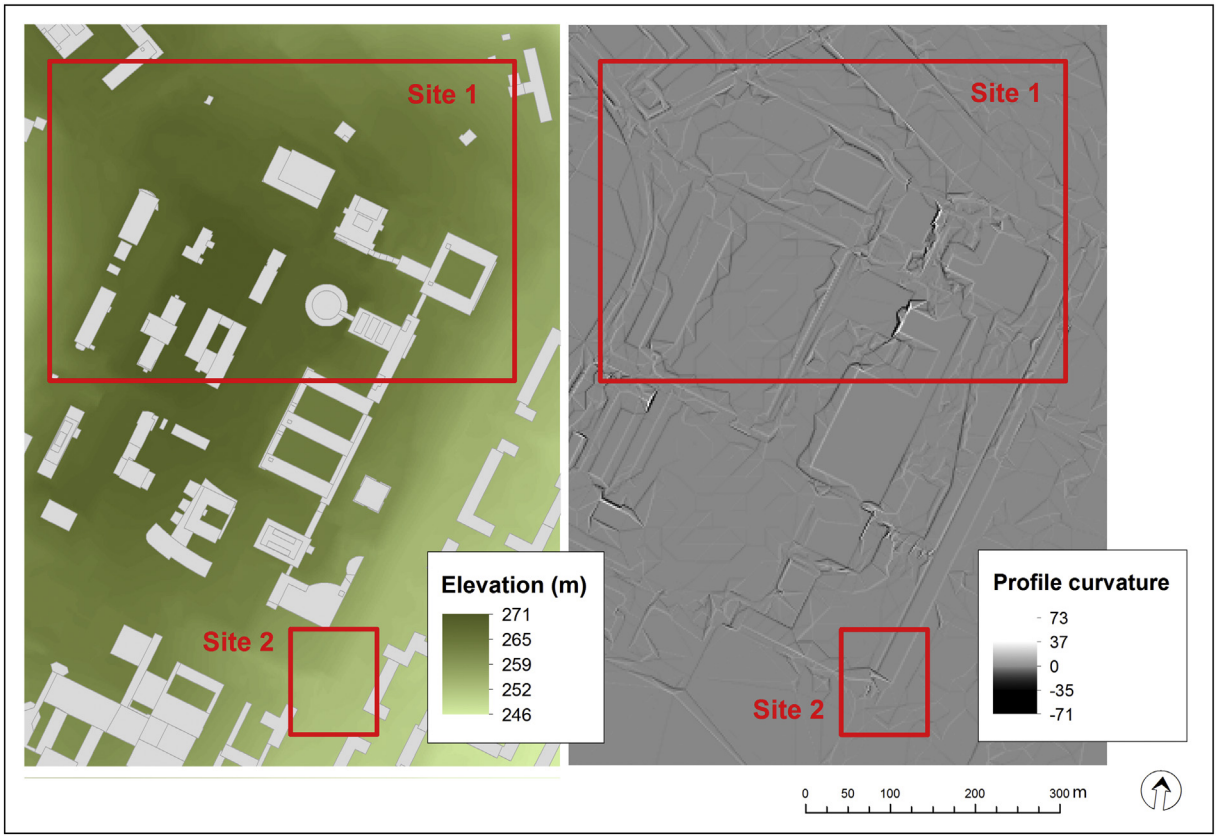

Appendix B. Preparing the DSMs for visibility analysis (Site 2)

The DSM with opaque obstacles merges the elevation of terrain and building height. The DSM with all obstacles merges the elevation of terrain, building height and vegetation height.

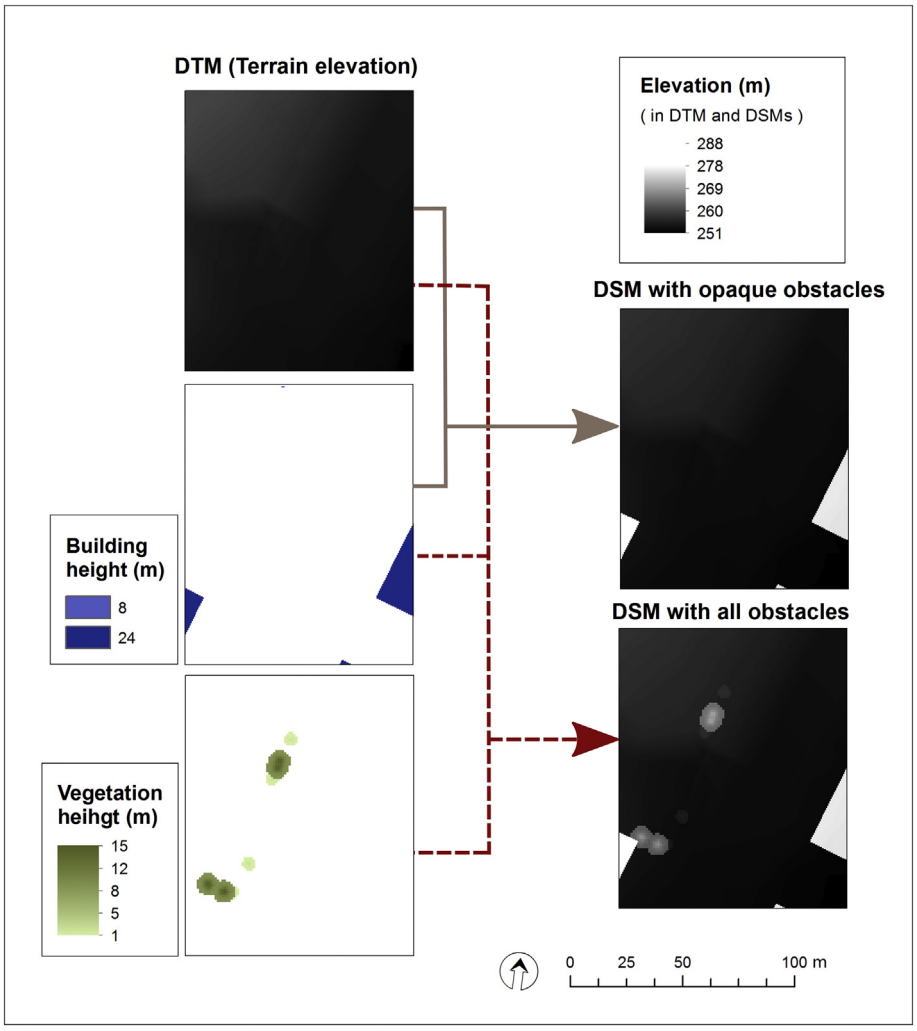

Appendix C. Implementation of the new method in ArcGIS (ModelBuilder)

Python script

Implementation of the new methodology in ArcGIS (Python script).

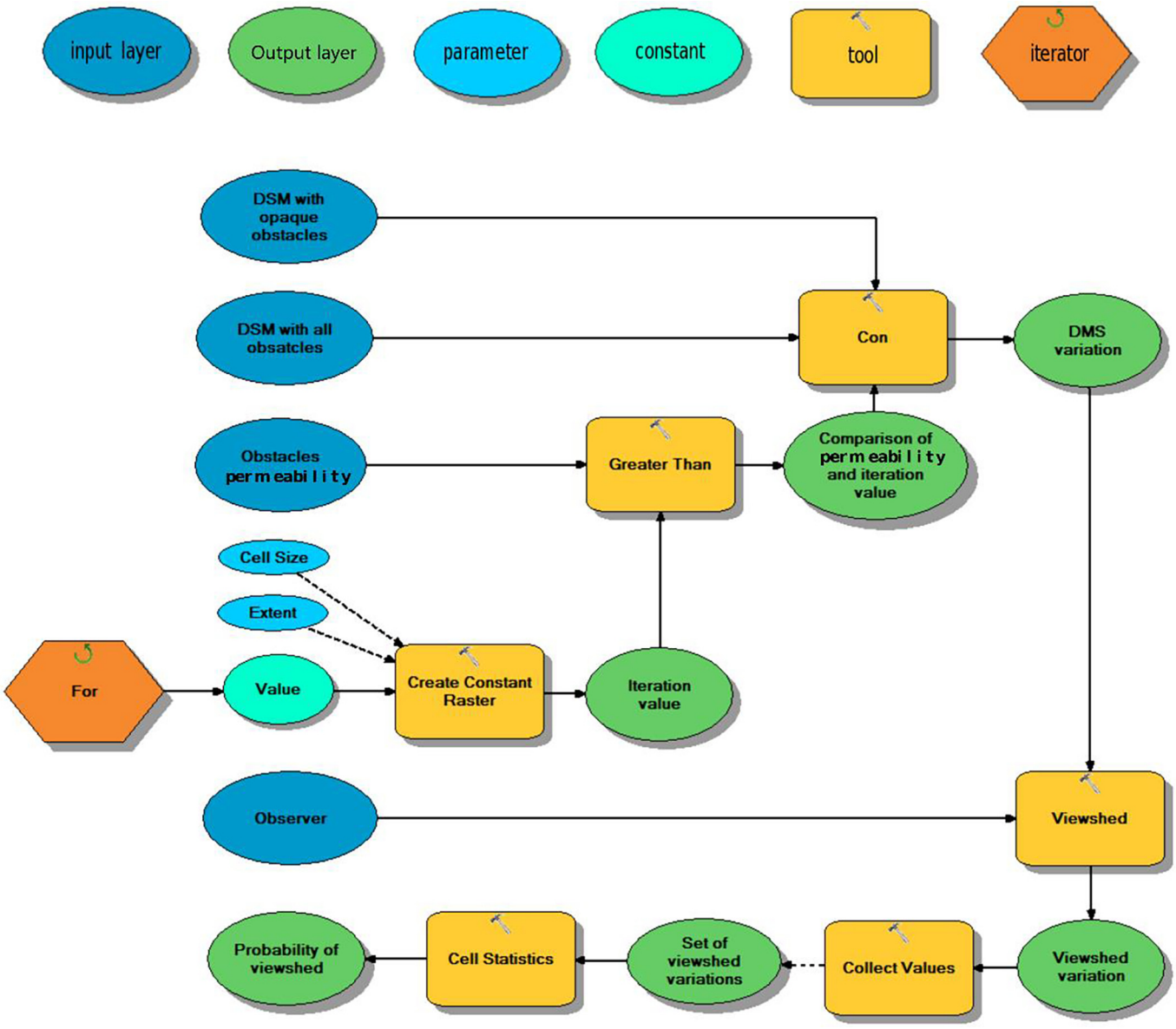

Appendix D. Result visibility at Site 2

The colour scale for probable visibility ranges is from darkest blue to lightest blue. Visible areas are not filled in. The colour scale was set in inverse order to highlight the rate of invisibility in the result. This picture shows the reduction in visibility behind the vegetation. Visibility reduction could also be perceived as the rate of shadows in a case where the source of light is placed in the observer's location. The picture on the right side shows the direction of view, which is displayed in Fig. 6.

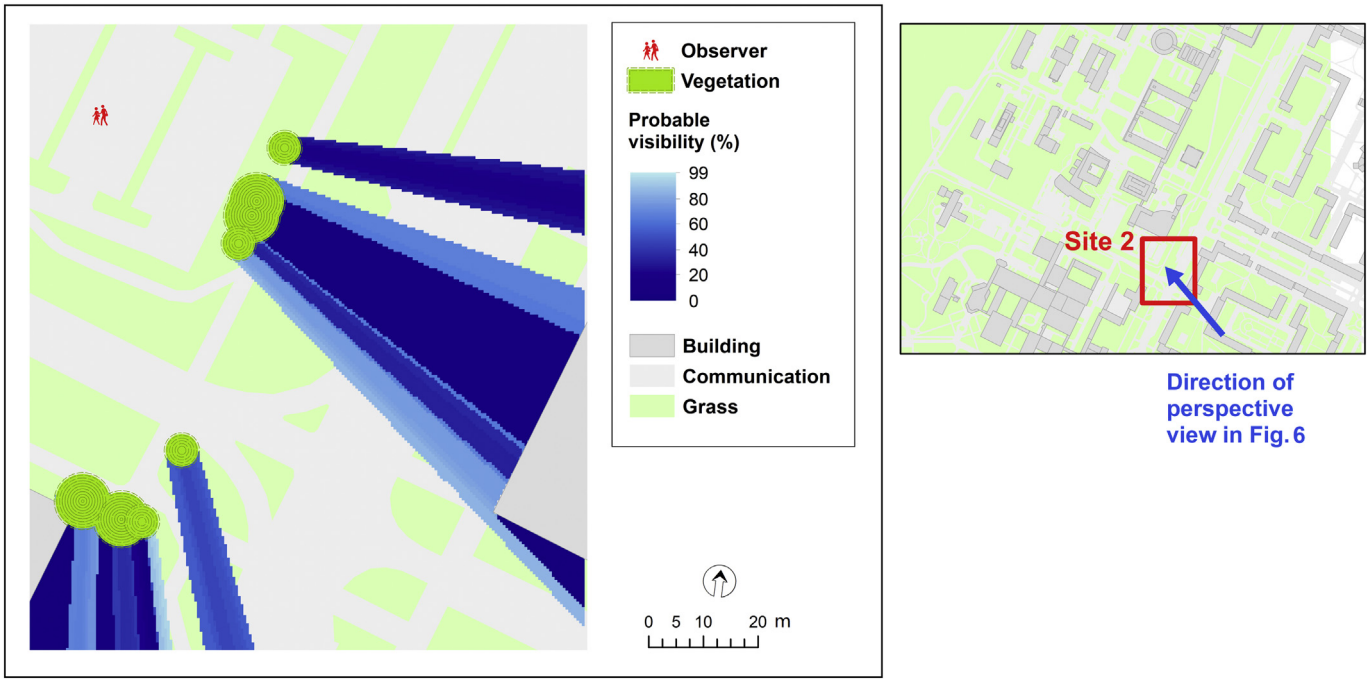

References

Arnot, R.H., Grant, K., 1981. The application of method of terrain analysis to functional land-capability assessment and aesthetic landscape appreciation. Landsc. Plan. 8 (3), 269–300.

Bartie, P., Reitsma, F., Kingham, S., Mills, S., 2010. Advancing visibility modelling algoriths for urban environments. Comput. Environ. Urban. Syst. 34 (6), 518–531.

Bartie, P., Reitsma, F., Kingham, S., Mills, S., 2011. Incorporating vegetation into visual exposure modelling in urban environments. Int. J. Geogr. Inf. Sci. 25 (5), 851–868.

Batty, M., 2001. Exploring isovist fields: space and shape in architectural and urban morphology. Environ. Plan. B 28, 123–150.

Benedikt, M., 1979. To take hold of space: isovists and isovist fields. Environ. Plan. B 6, 47–65. https://doi.org/10.1068/b060047.

Brabyn, L., 2015. Modelling landscape experience using "experions". Appl. Geogr. 62, 210–216.

Brandtberg, T., 2007. Classifying individual tree species under leaf-off and leaf-on conditions using airborne lidar. ISPRS J. Photogramm. Remote Sens. 61 (5), 325–340.

Burrough, P.A., 1986. Principles of geographical information systems for land resources assessment. Geocarto Int. 1 (3), 54.

Caha, J., Rasova, A., 2015. Line-of-sight derived indices: viewing angle difference to a local horizon and the difference of viewing angle and the slope of line of sight. Lect. Not. Geoinf. Cartogr. 211, 61–72.

Chamberlain, B.C., Meitner, M.J., 2013. A route-based visibility analysis for landscape management. Landsc. Urban Plan. 111 (1), 13–24.

Chang, Y., Habib, A., Lee, D., Yom, J., 2008. Automatic classification of lidar data into ground and nonground points. Int. Archiv. Photogr. Rem. Sens. Spatial Inf. Sci. 37 (B4), 457–462.

Chapman, H., 2006. Landscape Archaeology and GIS. The History Press Ltd., London, pp. 1–191.

Chen, Q., Baldocchi, D., Gong, P., Kelly, M., 2006. Isolating individual trees in a savanna woodland using small footprint LiDAR data. Photogramm. Eng. Remote. Sens. 72 (8), 923–932.

Cooper, G.R.J., 2005. Analysing potential field data using visibility. Comput. Geosci. 31 (7), 877–881.

Coops, N.C., Hilker, T., Wulder, M.A., St-Onge, B.A., Newnham, G.J., Siggins, A., Trofymow, J.A., 2007. Estimating canopy structure of douglas-fir forest stands from discrete-return LiDAR. Trees Struct. Func. 21 (3), 295–310. https://doi.org/10.1007/s00468-006-0119-6.

De Floriani, L., Magillo, P., 1999. Intervisibility on terrains. In: Longley, P.A., Goodchild, M.F., Maguire, D., Rhind, D.W. (Eds.), In Geographic Information Systems: Principles, Techniques, Managament and Applications, London, pp. 543–556.

De Floriani, L., Manzano, P., Puppo, E., 1994. Line of sight communication on terrain models. Int. J. Geogr. Inf. Syst. 8, 329–342.

De Floroani, L., Magillo, P., 1997. Visibility computation on hierarchical triangulated terrain models. GeoInformatica 1 (3), 219–250.

Domingo-Santos, J.M., De Villaran, R.F., Rapp-Arraras, I., Corral-Pazos de Provens, E., 2011. The visual exposure in forest and rural landscapes: an algorithm and a GIS tool. Landsc. Urban Plan. 101 (1), 52–58.

Duraciova, R., 2014. Implementation of the selected principles of the fuzzy set theory into spatial database systém and GIS. International Multidisciplinary Scientific GeoConference-SGEM Proccedings Bulgaria, pp. 627–634.

El-Sheimy, N., Valeo, C., Habib, A., 2005. Digital terrain modelling acquisition, manipulation, and applications. Proc. SPIE Int. Soc. Optical Eng. 9323 (2) 93232Q-93232Q-6.

ESRI, 2016. How Maximum Likelihood Classification Works. ArcMap Documentation. http://desktop.arcgis.com/en/arcmap/10.3/tools/spatial-analyst-toolbox/how-maximum-likelihood-classification-works.htm (accessed 6 May.2018).

ESRI, 2019. Multiple Ring Buffer. ArcGIS Pro Documentation. http://pro.arcgis.com/en/pro-app/tool-reference/analysis/multiple-ring-buffer.htm (accessed 18 February 2019).

Fisher, P.F., 1993. Algorithm and implementation uncertainty in viewshed analysis. Int. J. Geogr. Inf. Syst. 7 (4), 331–347.

Guth, P.L., 2009. Incorporating vegetation in Viewshed and Line-of-Site Algorithms. ASPRS/MAPPS 2009 Specialty Conference, San Antonio, Texas.

Hindsley, P., Hamilton, S.E., Morgan, O.A., 2013. Gulf views: toward a better understanding of viewshed scope in hedonic property models. Working Pap. 47 (3), 489–505. https://doi.org/10.1007/s11146-012-9365-0.

Immitzer, M., Atzberger, C., Koukal, T., 2012. Tree species classification with random forest using very high spatial resolution 8-band worldwiew-2 satelite data. Remote Sens. 4 (9), 2661–2693. https://doi.org/10.3390/rs4092661.

Kaucic, B., Zalik, B., 2002. Comparison of viewshed algorithms on regular spaced points. Proceedings of the 18th Spring Conference on Computer graphics (SCCG '02). ACM, pp. 177–183.

Kim, Y.H., Rana, S., Wise, S., 2004. Exploring multiple viewshed analysis using terrain features and optimisation technigues. Comput. Geosci. 30 (9–10), 1019–1032.

Klampfer, S., Mohorko, J., Cucej, Z., Chowdhury, A., 2011. Simulation of radio-visibility impact on the provided quality of service within the Wimax network. Informacije MIDEM Ljubljana 41 (3), 205–211.
Kloucek, T., Langer, O., Simova, P., 2015. How does data accuracy influence the reliability of digital viewshed models? A case study with wind turbines. Appl. Geogr. 64, 46–54.
Lange, E., 1990. Vista management in Acadia National Park. Landsc. Urban Plan. 19 (4), 353–376.
Lee, J., Stucky, D., 1998. On applying viewshed analysis for determining least-cost paths on Digital Elevation Models. Int. J. Geogr. Inf. Sci. 13 (8), 891–905.
Li, Z., Zhu, Q., Gold, Ch., 2005. Digital Terrain Modeling. Principles and Applications. 323. CRC Press.
Llobera, M., 2007. Modelling visibility through vegetation. Int. J. Geogr. Inf. Sci. 21 (7), 799–810.
Liu, L., Yhang, L.Q., Ma, J.T., Yhang, L., Yhang, X.M., Xiao, Z.Q., Yang, L., 2010. An improved line-of-sight method for visibility analysis in 3D complex landscapes. Sci. China Inf. Sci. 53 (11), 2185–2194.
Magoc, T., Kassin, A., Romero, R., 2010. A line of sight algorithm using fuzzy measures. 2010 Annual Meeting of the North American Fuzzy Information Processing Society (NAFIPS), Toronto, Canada. The Institute of Electrical and Electronics Engineers (IEEE), Piscataway, NJ.
Murgoitio, J.J., Shrestha, R., Glenn, N.F., Spaete, L.P., 2013. Improved visibility calculations with tree trunk obstruction modelling form aerial LiDAR. Int. J. Geogr. Inf. Sci. 27 (10), 1865–1883.
Nackaerts, K., Govers, G., Van Orshoven, J., 1999. Accuracy assessment of probabilistic visibilities. Int. J. Geogr. Inf. Sci. 13 (7), 709–721.
Natapov, A., Fisher-Gewirtzman, D., 2016. Visibility of urban activities and pedestrian routes: An experiment in a virtual environment. Comput. Environ. Urban. Syst. 58, 60–70.
Natural Resources Canada, 2015. Species Identification and Typing.
Nijhuis, S., Lammeren, R., Antrop, M., 2011. Exploring the Visual Landscape. Introduction. In: Nijhuis, S., Lammeren, R., Hoeven, F. (Eds.), Exploring the Visual Landscape. Advances in Physiognomic Landscape Research in the Netherlands. 2. Research in Urbanism Series, pp. 15–39 ISSN 1879-8217.
Ogburn, D.E., 2006. Assessing the level of visibility of cultural objects in past landscapes. J. Archeol. Sci. 33 (3), 405–413.
Paliou, E., 2011. The communicative potential of theran murals in late Bronze age Akrotiti: applying vewshed analysis in 3D townscapes. Oxf. J. Archaeol. 30 (3), 227–247.
Rana, S., 2006. Isovist Analyst - An Arcview extension for planning visual surveillance. ESRI International User Conference 7-11 August, 2006, San Diego, CA, USA. http://desktop.arcgis.com/en/arcmap/10.3/tools/spatial-analyst-toolbox/how-maximum-likelihood-classification-works.htm (accessed 30 Dcember 2020).
Sarnowski, L., Podgorski, Z., Brykala, D., 2018. 3D viewshed modelling using aerial photographs. Dissert. Cult. Landsc. Comm. 39 (1), 5–24. https://doi.org/10.30450/201801.
Smith, M.J., Goodchild, M.F., Longley, P.A., 2007. Geospatial analysis a comprehensive guide to principles techniques and software tools. Mandator 274–279.
Sunak, Y., Madlener, R., 2016. The impact of wind farm visibility on property values: A spatial difference-in-differences analysis. Energy Econ. 55, 79–91.
Supernant, K., 2014. Intervisibility and Intravisibility of rock feature sites: a method for testing viewshed within and outside the socio-spatial systém of the Lower Fraser Canyon, British Columbia. J. Archaeol. Sci. 50, 497–511.
Tandy, C.R., 1967. The Isovist method of landscape survey. In: Murray, C.R. (Ed.), Method of Landscape Analysis. Landscape Research Group, London, pp. 9–10.
Turner, A., Doxa, M., O'Sullivan, D., Penn, A., 2001. From isovists to visibility graphs: a methodology for the analysis of architectural space. Environ. Plan. B 28, 103–121.
Wang, J., Liu, X., Yang, X., Lei, M., Ruan, S., Nie, K., Miao, Y., Liu, J., 2014. Development and evaluation of a new digital photography visiometer system for automated visibility observation. Atmos. Environ. 87, 19–25.
Wassim, S., Thierry, J., Favier, E., 2011. 3D Urban Visibility Analysis With Vector GIS Data. Available at:. https://www.researchgate.net/publication/215999859_3D_Urban_Visibility_Analysis_with_Vector_GIS_Data (accessed 6 May, 2020).
Williamson, C.A., McLin, L.N., 2015. Nominal ocular dazzle distance (NODD). Appl. Opt. 54 (7), 1564–1572.
Wilson, J.P., Gallant, J.C., 2000. Terrain Analysis. Principles and Applications. John Wiley & Sons, Inc., p. 479.
Yang, P.P.Y., Putra, S.Y., Li, W., 2007. Viewsphere: a GIS based 3D visibility analysis for urban design evaluation. Environ. Plan. B 34 (6), 971–992.
Yu, T.X., Xiong, L.Y., Cao, M., Wang, Z.H., 2016. A new algorithm based on Region Partitioning for Filtering candidate viewpoints of a multiple viewshed. Int. J. Geogr. Inf. Sci. 30 (11), 2171–2187.
Zhang, K., Hu, B., 2012. Individual urban tree species classification using very high spatial resolution airborne multi-spectral imagery using longitudinal profiles. Remote Sens. 4, 1741–1757. https://doi.org/10.3390/rs4061741.